ELSEVIER

Journal of Alloys and Compounds 303–304 (2000) 360–363

Journal of
ALLOYS
AND COMPOUNDS

www.elsevier.com/locate/jallcom

Effects of thermal annealing on spectroscopic properties of Eu^{3+} in $Sr_{1-x}B_xNb_2O_6$ films

S.T. Li[a], G.K. Liu[a,]*, H. Liu[b], F.E. Fernandez[b]

[a]Chemistry Division, Argonne National Laboratory, Argonne, IL 60439, USA
[b]Department of Physics, University of Puerto Rico, Mayaguez, Puerto Rico 00681, USA

Abstract

Thermal annealing influence on properties of strontium–barium niobate (SBN) films doped with Eu^{3+} has been studied using laser spectroscopic methods. The Stark splittings of the $^5D_1$ state and all the ^7F_J states are well resolved only in the spectra from the annealed films, whereas the spectra of Eu^{3+} in the as-deposited film is similar to that in amorphous phases. Non-resonant fluorescence line narrowing (FLN) is observed only for the annealed film, which indicates a correlation between the energy levels of Eu^{3+} in inhomogeneous line broadening. Annealing-induced crystallization of the as-deposited film also increases the $^5D_0$ fluorescence lifetime and allows hyperfine spectral hole burning. © 2000 Elsevier Science S.A. All rights reserved.

Keywords: Eu^{3+} in SBN film; Laser spectroscopy; Thermal annealing

1. Introduction

Optical spectra of rare earth ions in solids carry ‘fingerprint’ information of local crystalline structure [1]. It is feasible to use laser spectroscopic methods to characterize local structure of rare earth ions in crystals and glasses. Particularly, for optical and laser materials doped with rare earth ions, laser spectroscopic studies provide information of local environments and insight into the relationship between electronic and structural properties that are not accessible with other methods.

Strontium–barium–niobate (SBN) is a promising material for many potential applications in optical switching [2,3] and optical computing with large electro-optic [4] and pyroelectric [5] coefficients and excellent photorefractive [6] properties. Especially, with crystal structure flexibility ($Sr_{1-x}Ba_xNb_2O_6$, $0.25 \leq x \leq 0.75$), SBN can be doped with many different chemical elements [7,8] to expand its applications. SBN films doped with rare earth ions are easy to make using such methods as laser deposition, but the films are not generally in crystalline structure. As a result, most optical properties of SBN in crystal form are lost. It is anticipated that thermal annealing may crystallize the as-deposited films and gain optical and spectroscopic properties comparable to that of SBN crystals. It was previously shown that thermal annealing of SBN films increased the refractive index by 12% and induced a red shift of effective absorption edge of 40 nm (H. Liu, unpublished data). Based on our experimental results, thermal annealing crystallizes the amorphous structure of the as-deposited films and significantly improved the spectroscopic properties of the doped Eu^{3+} ions.

The present work focuses on identification of spectroscopic changes of Eu^{3+}:SBN films after thermal annealing. Fluorescence line narrowing, lifetime measurements, and spectral hole burning were conducted on an as-deposited film and an identical film annealed at 1000°C for 2 h. Our results show that the annealing process significantly changed the microscopic environment of Eu^{3+} in the film, which strongly influences the spectroscopic and dynamic properties of f–f transitions in Eu^{3+}. Discussions are given to annealing-induced spectroscopic changes such as line shifts, line narrowing, energy level correlation and increase in the fluorescence lifetime of Eu^{3+}.

2. Samples and experimental details

SBN thin films doped with 0.5 wt% Eu were grown by reactive pulsed-laser deposition (PLD) on fused quartz substrates. $Sr_xBa_{1-x}Nb_2O_6$ targets with attempted composition $x=0.61$ were fabricated by cold-pressing and subsequent sintering of SBN powders previously obtained

---

*Corresponding author.

E-mail address: gliu@anlchm.chm.anl.gov (G.K. Liu)

0925-8388/00/$ – see front matter
PII: S0925-8388(00)00641-1

from solid-state reaction of high purity $SrCO_3$, $BaCO_3$ and Nb_2O_3 powders. The Eu_2O_3 dopant was added directly to the reacted SBN powders. Stoichiometry of the resulting targets was checked by X-ray diffraction (XRD) analysis, which showed that the peak pattern was consistent with the attempted composition. Metallic elements in SBN are not volatile at the substrate temperature we used. Hence, film composition was not expected to vary significantly from that of the target. Nevertheless, we verified this through Rutherford back-scattering spectroscopy (RBS) and particle-induced X-ray emission (PIXE) analysis of a sample grown on MgO. Metallic composition was in fact very close to that of the target. Eu concentration in the doped sample is too low to determine by RBS or PIXE. The expected concentration is approximately 0.5 wt%, which is the nominal concentration for the doped target. As determined by XRD analysis, the as-grown films were essentially amorphous. The annealed films were prepared by an annealing procedure in which the as-deposited films were heated at 1000°C for 2 h in flowing argon gas, then cooled to room temperature.

A Q-switched Nd:YAG laser pumped tunable dye laser with a band width of 0.3 cm^{-1} was the excitation source for recording fluorescence and excitation spectra. A monochromator with a spectral band pass of 0.3 cm^{-1} was used to select the fluorescence energy. The time-gated fluorescence emission was detected by a cooled photomultiplier connected to boxcar integrators. An argon ion laser pumped tunable CW dye laser was used for fluorescence line narrowing (FLN). In FLN measurements, two acoustic–optic modulators were used in series to covert the CW laser beam into pulse train. A mechanical chopper synchronized with the modulators was set in front of the monochromator to block residual light while passing Eu^{3+} fluorescence. With this time-resolved pump-then-detect method, scattered laser light was discriminated against by more than a factor of 10^{-6} when recording resonant fluorescence.

3. Results and discussion

The FLN fluorescence spectra were recorded at 4 K for both as-deposited and annealed Eu^{3+}:SBN films while the $^7F_0 \rightarrow {}^5D_0$ or $^7F_0 \rightarrow {}^5D_1$ transition of Eu^{3+} was excited. As shown in Fig. 1a, for Eu^{3+} in the as-deposited film, the spectrum is weak and broad, which indicates microscopic amorphous structure in the as-deposited film. In contrast, the spectrum of Eu^{3+} in the annealed film shown in Fig. 1b has well-resolved Stark splittings of ^7F_J ($J=0, 1\ldots4$) states, which provides clear evidence of crystalline structure in the annealed film.

It is well known that $^5D_0 \rightarrow {}^7F_2$ transition is hypersensitive to environment [9,10]. Such a transition tends to be more intense for Eu^{3+} at sites without inversion symmetry. It was shown in Fig. 1 that emission from the

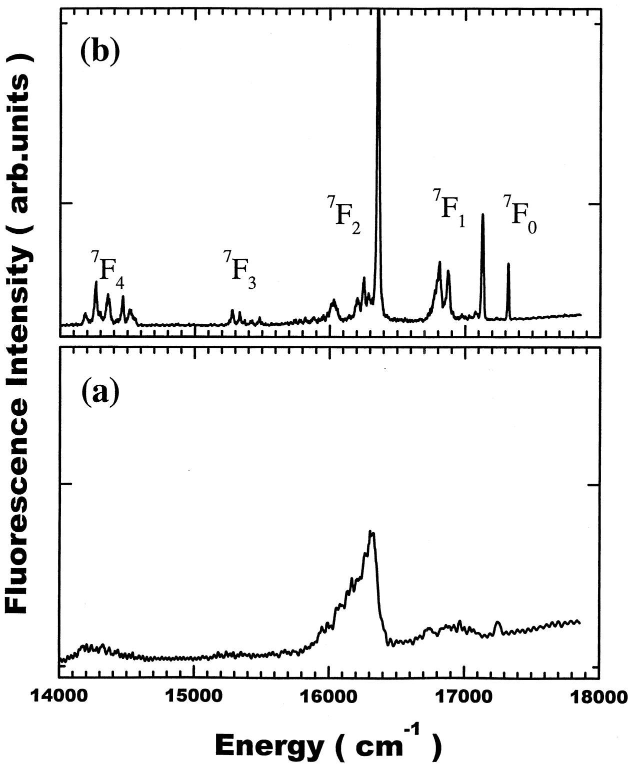

Fig. 1. Emission spectra of the $^5D_0 \rightarrow {}^7F_J$ ($J=0, 1\ldots4$) transitions of Eu^{3+} doped into (a) the as-deposited SBN film and (b) the annealed SBN film while the $^5D_1$ state of Eu^{3+} was excited at 4 K.

$^5D_0 \rightarrow {}^7F_2$ transition of Eu^{3+} in the annealed film was much stronger than that in the as-deposited film. Since Eu^{3+} ions may occupy two different sites in the SBN lattice, one with inversion symmetry and another without inversion symmetry. This result suggests that more Eu^{3+} ions were shifted to the asymmetric sites in the film after the thermal annealing and that the annealed film has a more uniform structure than the as-deposited film.

Fig. 2 illustrates the excitation spectra for the $^5D_0$ and $^5D_1$ states of the Eu^{3+} in the as-deposited film and the annealed SBN film, the fluorescence of the $^5D_0 \rightarrow {}^7F_2$ transition at 16 355 cm^{-1} was monitored. For the as-deposited film, lines of the $^7F_0 \rightarrow {}^5D_0$ and $^7F_0 \rightarrow {}^5D_1$ transitions were broad and no crystal field energy levels were resolved for the $^5D_1$ state. The two groups of asymmetric lines centered at 17 235 and 18 983 cm^{-1}, respectively, with inhomogeneous line-width of ~80 cm^{-1}. The inhomogeneous line broadening is similar to that for Eu^{3+} in glasses. Energy levels of the metal ion doped into the chemical complex may shift due to electron-cloud enlargement effect. For Eu^{3+}, the $^5D_0$ energy level can be used as a standard ruler to measure this effect [11] because the $^5D_0$ energy level no longer splits in crystal field. For the annealed film, the energy level of the $^5D_0$ of Eu^{3+} was measured to have a blue shift of 87 cm^{-1} and the corresponding spectral line centered at 17 322 cm^{-1}, with inhomogeneous line-width reduced to 30 cm^{-1}. The crystal

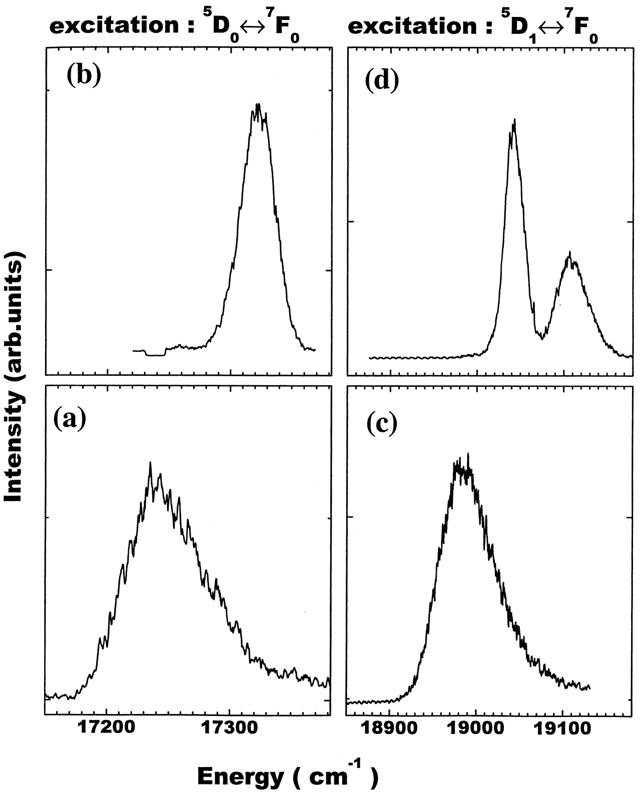

Fig. 2. Excitation spectra of the $^7F_0 \rightarrow {}^5D_0$ transition of Eu^{3+} in (a) the as-deposited SBN film and (b) the annealed SBN film by FLN method, and that of the $^7F_0 \rightarrow {}^5D_1$ of Eu^{3+} in (c) the as-deposited SBN film and (d) the annealed SBN film. The spectra were obtained at 4 K, and the emission of the $^5D_0 \rightarrow {}^7F_2$ transition of Eu^{3+} was monitored.

field splitting of the $^5D_1$ excited state of Eu^{3+} was observed in the annealed film as well as the ^7F_J multiplets. Two lines center at 19 088 and 19 026 cm^{-1}, respectively, with an average blue shift of 65 cm^{-1} in comparison with that in the as-deposited film.

In general, sharp lines of crystal field splitting provide evidence of crystalline structure in solids. The 30-cm^{-1} inhomogeneous line width of the $^7F_0 \rightarrow {}^5D_{0,1}$ transitions for Eu^{3+} in the annealed sample suggests that there is still significant structure disorder. Usually, the inhomogeneous linewidth of trivalent rare earth ions in crystals is less than 10 cm^{-1}. With a non-resonant FLN method, we observed that the spectral line of the $^5D_0 \rightarrow {}^7F_2$ transition centered at 16 355 cm^{-1} shifted as the excitation wavelength altered within the $^7F_0 \rightarrow {}^5D_0$ transition for the annealed film. Fig. 3 shows that the center of the spectral line of the $^5D_0 \rightarrow {}^7F_2$ transition of Eu^{3+} varies linearly as the excitation wavelength varied across the $^7F_0 \rightarrow {}^5D_0$ transition of Eu^{3+} in the annealed SBN film. No such behavior was observed for the as-deposited film and the fluorescence line center and shape are independent of excitation wavelength. According to the theory of inhomogeneous line broadening in solids [12,13], this correlation of inhomogeneous broadening between the energy levels of the excited states suggests that the disorder is macroscopic in the annealed film and microscopic in the as-deposited film. Macroscopic broadening reflects the nature of ions having similar local environments but lacking long range order.

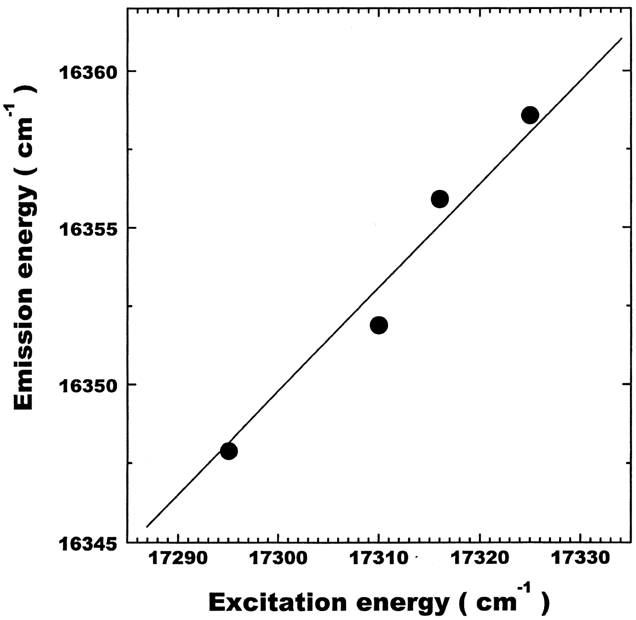

Fig. 3. Correlation between the $^7F_0 \rightarrow {}^5D_0$ excitation and the $^5D_0 \rightarrow {}^7F_2$ emission as the laser energy is varied across the inhomogeneous line of Eu^{3+} in the annealed SBN film.

Fig. 4 shows the fluorescence decay of the $^5D_0 \rightarrow {}^7F_2$ transition, while the $^5D_0$ emitting state was directly excited. The measured lifetime of 0.8 ms for the $^5D_0$ state of Eu^{3+} in the as-deposited film is very close to that of 1 ms for Eu^{3+} in glass [14]. For the annealed film, the

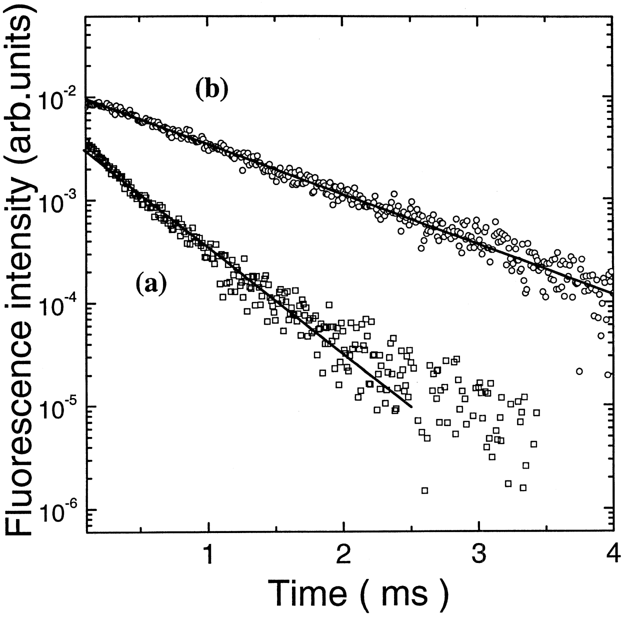

Fig. 4. Fluorescence decay of the $^5D_0 \rightarrow {}^7F_2$ transition of Eu^{3+} in (a) the as-deposited SBN film and (b) the annealed SBN film after excitation of the $^5D_1$ state at 4 K.

lifetime measured from the fluorescence decay was 2.2 ms, which is in reasonable agreement with that (1.8~5 ms) for Eu^{3+} doped into crystals [15]. The change in lifetime is because non-radiative relaxation is significantly greater in amorphous phases than in crystals [16]. While the decay curve for Eu^{3+} in the annealed film is single exponential, the fluorescence decay is non-exponential in the as-deposited film. The non-exponential fluorescence decay for the as-deposited film indicates that microscopic structure in the as-deposited film is more inhomogeneous compared with that in the annealed film. This result also supports the argument that Eu^{3+} ions in the annealed SBM film occupy one crystal lattice site.

As an additional evidence of structure change-induced spectroscopic property improvement, hyperfine spectral hole burning in the $^7F_0 \rightarrow ^5D_0$ transition of Eu^{3+} was observed only in the annealed film. The hole depth was measured to be about 30% of the fluorescence intensity. The homogeneous linewidth of the $^5D_0$ level of the Eu^{3+} was about 70 MHz at 4 K according to the measured spectral hole width. Anti-holes were observed in two sides of the primary hole but the hyperfine energy levels cannot be resolved because of the broad hole width.

4. Conclusions

We have performed laser spectroscopic characterization of thermal annealing of amorphous SBN films doped with Eu^{3+}. Our experimental results show drastic differences of spectroscopic characteristics of Eu^{3+} in between the as-deposited film and the annealed SBN film. The inhomogeneous linewidth and excited state lifetime were measured for qualitative determination of the degree of structure disorder. For the as-deposited film, the results are consistent with the amorphous characteristics of its microscopic structure. Thermal annealing changes the film's microscopic structure to crystalline lattice. As a result, the spectroscopic properties of the f–f transitions are significantly altered. The sharp crystal field levels appear in the fluorescence and excitation spectra of Eu^{3+} in the annealed SBN film. There is clear evidence of macroscopic inhomogeneous line broadening in the annealed film. The fluorescence decay measurements also show evidence of crystallization induced by the thermal annealing. Moreover, the annealed Eu^{3+}:SBN film exhibits a strong hyperfine spectral hole burning effect. Given that significant improvements and changes in the Eu^{3+} spectroscopy and dynamics can be achieved by thermal annealing, SBN films containing rare earth ions may have strong potential in optical applications.

Acknowledgements

This work was performed under the auspices of the Office of Basic Energy Sciences, Division of Chemical Sciences, US Department of Energy under contract number W-31-109-ENG-38.

References

[1] C. Görller-Walrand, K. Binnemans, in: K.A. Gschneidner Jr., L. Eyring (Eds.), Handbook on the Physics and Chemistry of Rare Earths, Vol. 23, North-Holland, Amsterdam, 1996, pp. 121–283, Chapter 155.

[2] P. Guenter, J.-P. Huignard (Eds.), Photorefractive Materials and Their Applications I and II, Vols. 61–62, Springer, Berlin, 1988–1989.

[3] A. Gerwens, M. Simon, K. Buse, E. Kraetzig, Opt. Commun. 135 (1997) 347.

[4] P.V. Lenzo, E.G. Spencer, A.A. Ballman, Appl. Phys. Lett. 11 (1967) 23.

[5] A.M. Glass, J. Appl. Phys. 40 (1969) 4699.

[6] K. Megumi, H. Kozuka, M. Kobayashi, Y. Furuhata, Appl. Phys. Lett. 30 (1977) 631.

[7] M.D. Ewbank, P.R. Neurgaonkar, W.K. Cory, J. Feinberg, J. Appl. Phys. 62 (1987) 378.

[8] K. Buse, U. van Stevendaal, R. Pankrath, E. Kraetzig, J. Opt. Soc. Am. B 13 (1996) 1461.

[9] B.R. Judd, Phys. Rev. 127 (1962) 750.

[10] F.S. Ofelt, J. Chem. Phys. 37 (1962) 511.

[11] P. Caro, O. Beaury, E. Antic, J. Phys. 37 (1976) 671.

[12] P. Caro, O. Beaury, E. Antic, J. Phys. 37 (1976) 671.

[13] G.K. Liu, J. Huang, J.V. Beitz, Phys. Rev. B 48 (1993) 13351.

[14] C. Brecher, L.A. Riseberg, Phys. Rev. B 13 (1976) 81.

[15] R.M. Macfarlane, R.M. Shelby, in: A.A. Kaplyanskii, R.M. Macfarlane (Eds.), Spectroscopy of Solids Containing Rare Earth Ions, Elsevier, Amsterdam, 1987, p. 51.

[16] P.M. Selzer, D.L. Huber, D.S. Hamiton, W.M. Yen, M.J. Weber, Phys. Rev. Lett. 36 (1976) 813.